Deep Potential Development of Transition-Metal rich Carbides

Tyler McGilvry-James[1]*, Bikash Timalsina[2], Marium Mostafiz Mou[1], Ridwan Sakidja[1]

1. *Physics, Astronomy, and Materials Science Department, Missouri State University, 901 S. National Avenue, Springfield, Missouri 65897, US*
2. *Mechanical Engineering Dept., University of Virginia, 351 McCormick Road, Charlottesville, VA 22904*

ABSTRACT:

In this study we developed DeepPot-SE type potentials according to the High Entropy Strategy for $Cr_{23}C_6$, $Fe_{23}C_6$, $W_{23}C_6$, and $Mo_{23}C_6$ systems. Predictive molecular dynamics are then conducted according to various elastic and mechanical properties. Training dataset accuracy is confirmed both numerically and visually. Elastic constants, Poisson Ratio, and bulk modulus are determined and compared to literature with percent errors ranging between 0.45-13.33%. Ground-state lattice constants yield 0.111-1.375% percent error. Linear lattice constant thermal expansion trends are found from 300-1500K as expected. Melting behaviors with clear melting points are observed for each binary. The Birch-Murnaghan Equation of State is suitably fit, providing additional verification of the bulk modulus calculations. Polycrystalline thermal stability is also verified for each binary potential.

CONTRIBUTIONS:

Support from the National Energy Technology Laboratory (Grant No. FE0031554) is gratefully acknowledged. We also acknowledge the computational resources from the National Energy Research Scientific Computing Center (NERSC) through the ERCAP0018177 allocation.

Introduction

Nickel-based superalloys are the current state of the art materials used for a wide range of power generation applications, ranging from turbine engines to powerplants, which is potentially subject to creep deformation under aggressive environments.[1] A persistent challenge as far as the materials design as concerned has been the inability to accurately predict creep deformation, due to the complexity in building the key issue of modeling of polycrystalline structures and the grain boundaries.[1, 2]. Well-known precipitates, which are critical to creep resistance, are typically comprised of the mixtures of transition-metal rich carbide phases: binaries or higher order forms of $M_{23}C_6$, where M stands for transition metals (e.g. Cr, Mo, W, Fe, etc)[3] Thus, accurately modeling the properties of precipitates is a key issue in building up a more comprehensive modeling in properly predicting creep deformation.

The electronic structure calculations using Density Functional Theory (DFT) codes such as the Vienna Ab-initio Software Package (VASP) [4-6]have long been capable in predicting fundamental properties of the carbide systems in general, but these calculations necessitate expensive computational resources. Finite temperature *ab-initio* calculations have also been applied to capture accurate snapshots of the system, however the total observable timescale for these types of calculations is quite limited due to the necessarily small timestep (~0.1ps) required in an already small simulation box. Thus, scalable classical molecular dynamics (MD) simulations that can duplicate the *ab-initio* accuracy would be highly desirable. In this study, we have developed the deep potentials designed for classical MD simulations for a series of $M_{23}C_6$ phases by utilizing the raw data from DFT-based finite temperature MD simulations. The methodology has been shown to successfully model a wide range of bulk properties [7]. In this case, a powerful backbone of Graphics Processing Unit (GPU) parallelized Tensorflow and an easy-access python interface of DeePMD-kit has facilitated an effective mobilization of large *ab-initio* datasets and generate a series of reasonably accurate and predictive potentials.

Computational Methodology

Ab-initio Data Generation

Initial configurations for first principle molecular dynamics (FPMD) are based on *cif* formatted crystallographic data from the Materials Project (mp-723). Training data is generated for each binary carbide according to the recommendations of VASP documentation for canonical ensemble (NVT) FPMD sampling, including recommended GPAW pseudopotentials.[4-6, 8-10] A Nose-Hoover thermostat is selected given that the Langevin frictional coefficients need not be employed for these systems. To ensure accurate sampling, and given that explicit relaxation data is not sampled, a sufficient kinetic energy cutoff of 400eV is chosen for each binary, being the largest of each species from selected pseudopotentials. An SCF iteration criterion of 1E-5 eV and precision is set to *accurate*. Finally, given a large cell size of 116 atoms, for efficiency of data generation real space projectors and distributions are enabled with a *1x1x1* KPOINTS grid.

The general strategy we employed here, which we coined, as the "high entropy strategy" which is a sampling technique that attempts to maximize a statistical variation in terms of volumetric/pressure and energetic environments possible of the phase of interest. The total phase-space for the $M_{23}C_6$ phase or melt is sampled in a necessarily diverse fashion by expanding a wide of simulation temperatures and volumes for a given temperature. Such choices in training allow the potential to accommodate various local environments during predictive molecular dynamics. Temperatures are selected according to table 1 and roughly the corresponding number of frames are generated. The input cell volume is then scaled to permit negative or positive overall virial states as well as the near-equilibrium simulations of varying degrees. We also incorporate diversification on compositions through the inclusion of hypothetical $M_{23}C_6$-prototype "$C_{23}M_6$" structures constructed by swapping all metal and carbon positions. (Supporting information are provide in the supplementary section). Such an approach can also potentially extended to higher order systems, by sampling, as a proof of concept, the high entropy alloy (HEA) carbide compositions of $M_{23}C_6$ phase which comprise of a relatively equal amount of transition metals . Similarly, in this case, we also employed the same strategy of exploring the various temperature-volume domains with more extensive compositional variations explored by randomizing the transition metal sites with $M_{23}C_6$. In each sampled set of trajectories, the early frames are purposely truncated and not used for training or testing purposes due to erroneous energy considerations due to the typically initially randomized velocity assigned thereby improving overall data quality. An average sampling of ~32000 frames per binary training set serves to reduce the extent of overfitting, improve the

generalizability of the model, and extend the range and distribution of phase-space sampling.[7]

DeePMD-Kit Parameter Selection

DeePMD-kit is used to generate Deep Potential – Smooth Edition (DeepPot-SE) neural networks.[11, 12] Radial and angular descriptors from input frames are considered to enhance reliability of predicted elastic properties. Further training parameters are then decided upon by previous literature and the considerations of potential applications. Therefore, in accordance with Liang et al, three-layer embedding and fitting networks composed of [25, 50, 100] and [240, 240, 240] neurons respectively are employed.[13, 14] A cutoff radius of 5.8Å ensures significant neighbor interactions of up to the third nearest neighbor from each training dataset. Non-zero virial prefactors are used to explicitly train the elastic information contained within the datasets. The initial and final energy, force, and virial prefactors are [0.02, 1], [1000, 1], and [100, 1] are used for five million training steps.[13, 14]

Results

Model Accuracy

Average RMSE training values total to 9.9 eV, with contributions of 8.219E-3 eV, 4.778E-1 eV/Å, and 2.618E-2 eV from energy per atom, force, and virial per atom respectively after ~400,000 training steps. These training errors are within the same order of magnitude of other published literature.[13] Furthermore, given inclusion of virial perfectors in this calculation, it is natural that the total RMSE error is larger than seen in other literature, where only force and energy are used for training. Energy and force matching are linear in nature, with a correlational coefficient of 0.998 and 0.925 respectively. Figure 1 (Supporting information S1 for energy, force, and virial fitting visualization with other systems training sets) shows that reproduced *x*-forces are bulkier, while energy and virial fittings are tight; however, the linear-regression on forces – by slope and correlational coefficient – of any chosen axis is linear in nature. Such near-linear relationships indicate the model well reflects trained data Numerical RMSE outputs demonstrate that the model is representative of the trained *ab-initio* datasets. Low final error values further emphasize numerically the accuracy of the potential upon the diverse training set as shown in Figure 1abc. Testing upon an independent and un-trained temperature FPMD dataset at 2500K reflects average RMSE errors for energy per atom, force, and virial per atom as 1.86E-2, 5.69E-1, and 8.11E-2 respectively. These testing results indicate that the potential accurate represents intermediate untrained temperatures. Additionally, potential robustness is reflected in molecular dynamic simulations which sample untrained environments and properties – serving to additionally confirm overfitting has not occurred.

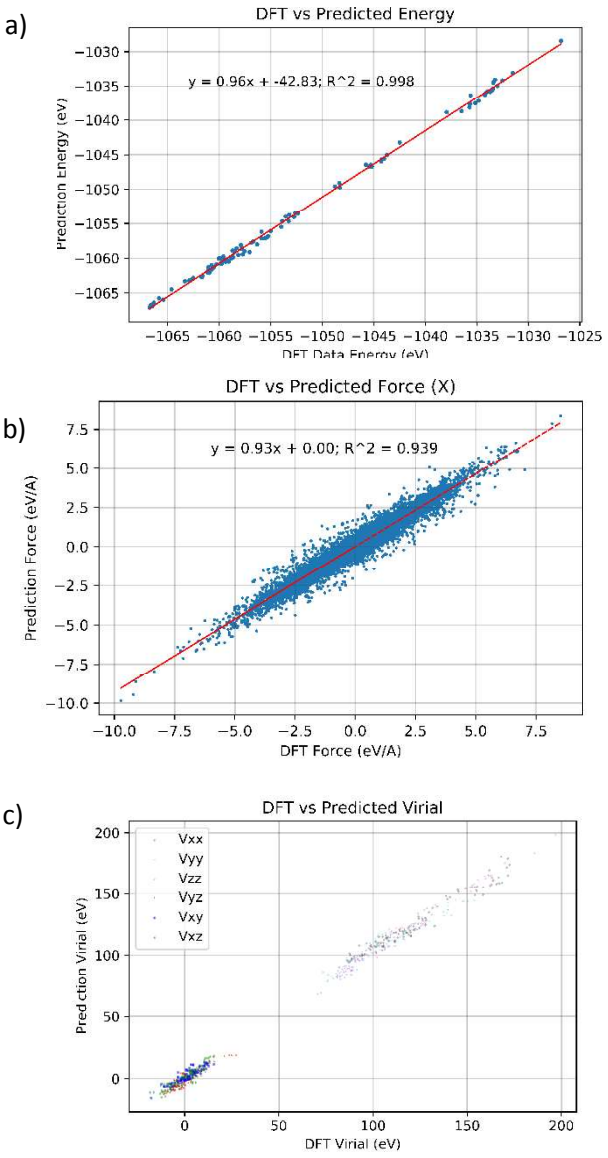

Fig 1(a,b,c) Energy, force and virial matching of $Cr_{23}C_6$ as predicted by the deep potentials in y axis versus training-DFT data (x axis).

Table 1. Selection of *ab-initio* data used for model training. Each binary is sampled at 2000K, 2900K, 3500K, 4000K, 4500K, and 5000K at various volumes to represent a range of force phase-space in sampling.

Carbide	Scheme	Frames	Carbide	Scheme	Frames
$Cr_{23}C_6$	5000K NVT Volumes	~3000	$Fe_{23}C_6$	5000K NVT Volumes	~3000
	4500K NVT Volumes	~3800		4500K NVT Volumes	~3800
	4000K NVT Volumes	~3500		4000K NVT Volumes	~3500
	3500K NVT Volumes	~10000		3500K NVT Volumes	~10000
	2900K NVT Volumes	~10000		2900K NVT Volumes	~10000
	2000K NVT Volumes	~2500		2000K NVT Volumes	~2600
$W_{23}C_6$	5000K NVT Volumes	~3000	$Mo_{23}C_6$	5000K NVT Volumes	~3000
	4500K NVT Volumes	~3800		4500K NVT Volumes	~3800
	4000K NVT Volumes	~3500		4000K NVT Volumes	~3500
	3500K NVT Volumes	~10000		3500K NVT Volumes	~10000
	2900K NVT Volumes	~10000		2900K NVT Volumes	~10000
	2000K NVT Volumes	~2900		2000K NVT Volumes	~2500

Elastic Properties

Accurate prediction of elastic properties is necessary for eventual modeling of creep deformation behavior. Elastic constants and associated properties (η, K) are determined using LAMMPS and compared to established literature with close matching. Therein developed potentials accurately reflect desirable elastic properties of the $M_{23}C_6$ phases: ground-state elastic constants, Poisson Ratio, and Bulk Modulus. Notably, the elastic properties are not explicitly sampled in the training dataset in anyway and only NVT simulations are used; however, accurate predictions are still made.

The $Cr_{23}C_6$ average percent errors across all elastic constants range between 5.31-6.53% with close η and K agreement.[15, 16] $Fe_{23}C_6$, $W_{23}C_6$, and $Mo_{23}C_6$ remain in similar contention averaging 6.64%, 1.20%, and 7.05% respectively with general agreement between η and K (Supporting information lists the complete tables of calculated elastic properties from MD).[15, 16] Therefore, DeepPot-SE type potentials trained can accurately predict the ground-state elastic constants and bulk elastic properties of interested binary systems within *ab-initio* ranges

Table 2. Computed elastic constants, Poisson ratio, and bulk modulus predicted by trained models compared to first-principles calculations and experimental results listed below.

Carbide	C_{11} (GPa)	C_{12} (GPa)	C_{44} (GPa)	η	K (GPa)
$Cr_{23}C_6$	482.06	226.82	145.67	0.3199	311.898
	472.15[15]	198.00[15]	137.44[15]	0.3141[15]	298.427[15]
	471.6[16]	215.7[16]	135.1[16]	0.31[16]	301.0[16]
	477[17]	198[17]	137[17]	0.30[17]	291[17]
$Fe_{23}C_6$	535.92	254.64	140.35	0.39231	356.557
	490.7[16]	255.9[16]	133.8[16]	0.34[16]	334.2[16]
$W_{23}C_6$	512.88	255.84	134.29	0.3328	341.519
	510.38[15]	252.59[15]	136.12[15]	0.3261[15]	338.521[15]
$Mo_{23}C_6$	455.20	204.52	101.86	0.3416	267.76
	457.24[15]	220.09[15]	113.51[15]	0.3279[15]	299.138[15]

a

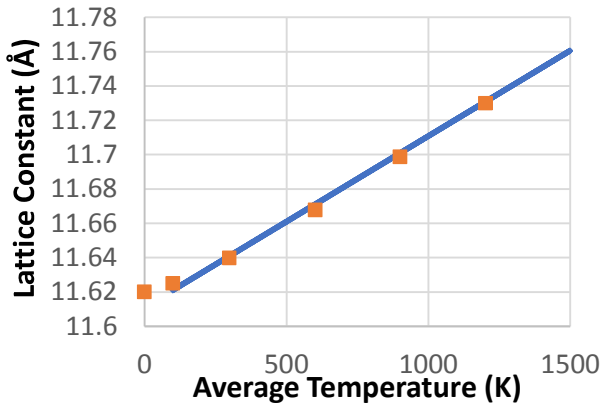

b)

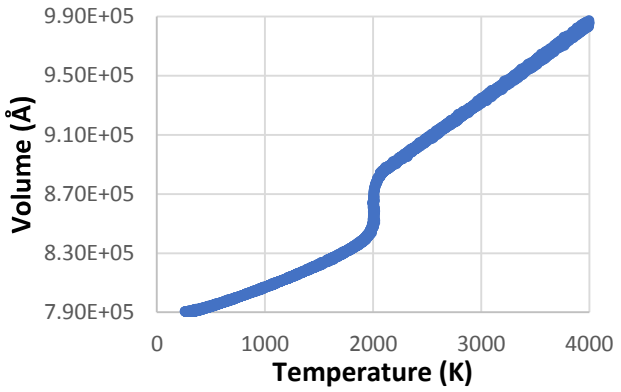

c

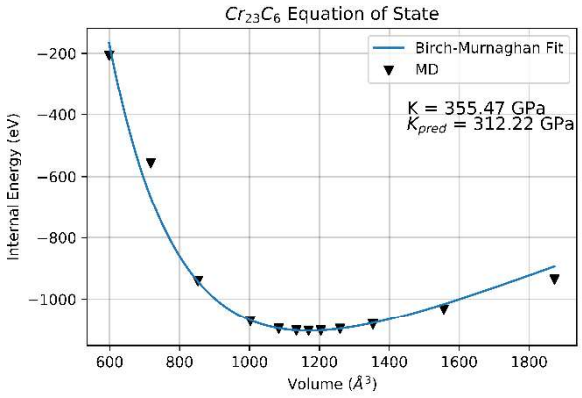

FIG. 2(a,b,c). **(a)** Predicted average lattice parameters of $Mo_{23}C_6$ varying by temperature (black) and the linear regression on temperatures greater than 100K (red) with correlation coefficient. **(b)** Upper-bound melting point determination of $Fe_{23}C_6$ with volume by temperature. **(c)** MD determined internal energy by structure volume using potential with corresponding Birch-Murnaghan fitting and determined bulk modulus, K

Mechanical Properties

Mechanical validations of developed potentials encompass temperature dependent lattice constants, melting point behavior, Birch-Murnaghan Equation of State, and polycrystalline stability. Thermal stability is given into the ultra-high temperature range and various thermo-mechanical properties are accurately modeled. The five-component potential (Fe-Cr-Mo-W-C) is developed according to the High Entropy Strategy and trained with varying randomized transition-metal compositions in the $M_{23}C_6$ geometry. The potential is successful at simulating a thermally stable supercell in the low-mid temperature regimes.

Thermal expansion is tested using alternating stages of heating and equilibration during NPT simulations. Figure 2a (The supporting information provides the plots of average lattice parameters as a function of temperature for each binary system) reveals expected linear trends for the carbides in the low-temperature range (300-1500K) as validated by high correlational coefficients in linear regression. Such qualitative behavior is expected in this temperature regime as the structure is stable and must exhibit low anharmonicity.

Relaxing each carbide to the ground-state yields the cell volume and lattice parameters. Subsequently the expected cubic structure is properly replicated with associated lattice parameter percent errors for $Cr_{23}C_6$, $Fe_{23}C_6$, $W_{23}C_6$, and $Mo_{23}C_6$ at the ground-state of 0.111%, 0.438%, 0.354%, and 0.740% respectively relative to Puja Adhikari et al. but vary to 1.375% and 0.891% when compared to the results of Liu et al for the $Cr_{23}C_6$ and $Fe_{23}C_6$ systems. [15, 16]. Such estimations lie clearly within the contention of *ab-initio* calculations.

Melting point signals are exhibited for each binary system. Figure 2b (The supporting information provides various NPT tests with corresponding volume by temperature graphs) displays such behavior for the $Fe_{23}C_6$ system as determined in NPT simulation with 5E-4 picosecond timesteps for an initial equilibration of 1000 steps and additional heating for 49000 steps to 3500K. The system exhibits linear thermal expansion both before and after the phase transition, with a near-

discontinuous change in volume at the melting point. Therefore, MD indicates a melting point signal at 2000K. Signal quality from MD varies between chosen transition metal; however, supplemental material supports further transparent melting point signals across all trained binary systems.

To evaluate the energy accuracy of the deep potentials, we calculated the variation of the total energy as a function of various volumes for all the binary carbides (see supplementary data for the results). Subsequent fitting is then conducted according to the Birch-Murnaghan Equation of State. The supporting information provides the complete graphs of each binary Equation of State, predicted bulk modulus, and functional fitting by fixing the initial volume as that determined by prior cell relaxation.[18, 19] Figure 2c shows a sufficient fitting with the predicted bulk modulus of 355.47 GPa for the $Cr_{23}C_6$ system, with a relatively small difference of to both those reported by the references and calculated by LAMMPS.[15-17]

To test the application of the deep potential, we used Atomsk which employs a Voronoi tessellation algorithm[20] to generate the hypothetical polycrystalline carbide phase and then tested the thermal stability of the structures. The NPT simulation with 12271 atoms occupying three grains exhibits thermal stability. As a proof of concept, we also developed the higher order potentials and tested the deep potentials onto the hypothetical HEA carbide system of $(Fe,Cr,Mo,W)_{23}C_6$. demonstrated a high thermal stability for the polycrystalline HEA carbides (see the supplementary data). Further details on the results of the potential development of the HEA carbides will be given in a subsequent publication, but by utilizing the same high entropy strategy, we have been able to demonstrate here a fairly simple but promising strategy to develop the deep potentials capable in modeling a variety of physical properties of various transition metal-carbide systems. Furthermore, polycrystalline stability provides a strong indication on the potential generalizability to model untrained environments by exposing atoms to various geometries at the grain boundary.

Conclusion

The high entropy strategy is largely successful at developing DeepPot-SE type potentials for transition-metal rich carbides of the form $M_{23}C_6$ where M is a transition metal. Potentials are capable of predictive molecular dynamics relating to the stability, elasticity, and mechanical properties of the interested structures achieved by sampling a variety of temperatures and volumes according to canonical ensemble *ab-initio* DFT data. Elastic constants are reproduced within the range of DFT literature with tolerable error and lattice parameters are reproduced with near negligible error, without explicit sampling of shear deformation structures.

The current study suggests the expansion of development to other transition-metal carbides of various compositions, especially those which are precipitates of Ni-based superalloys. Mechanical predictability will be further enhanced through extended phase-space variation in accordance with the High Entropy Strategy and larger training datasets. Thereby extended and enhanced investigation of transition-metal rich carbide phases and high entropy alloys will unlock the ability to model more complex environments such as the grain boundaries of Ni-based superalloys. Future work will then expose the nature of creep deformation in these all-important commercial alloys.

Supporting Information

Supporting data is provided in the supplementary section. Similarly, the datasets, potentials, and results can also be accessed from at https://github.com/sakidja/deep_potentials/ or through personal inquiry.

Acknowledgements

Support from the National Energy Technology Laboratory (Grant No. FE0031554) is gratefully acknowledged. We would also like to express our gratitude to NERSC (ERCAP0018177) for providing the supercomputer resource.

Conflict of Interest

On behalf of all authors, the corresponding author states that there is no conflict of interest.

References

1. Smith, T.M., et al., *Creep deformation mechanism mapping in nickel base disk superalloys.* Materials at High Temperatures, 2016. **33**(4-5): p. 372-383.
2. Pinky, S. *Molecular Dynamics Study of Creep Deformation in Nickel-based Superalloy*. 2019.
3. Gvs, M., *Characterization of Intermetallic Precipitates in Ni-Base Alloys by Non-destructive Techniques*. 2016.
4. Kresse, G. and D. Joubert, *From ultrasoft pseudopotentials to the projector augmented-wave method.* Physical Review B, 1999. **59**(3): p. 1758-1775.
5. Kresse, G. and J. Furthmüller, *Efficiency of ab-initio total energy calculations for metals and semiconductors using a plane-wave basis set.* Computational Materials Science, 1996. **6**(1): p. 15-50.
6. Kresse, G., *Ab initio molecular dynamics for liquid metals.* Journal of Non-Crystalline Solids, 1995. **192-193**: p. 222-229.
7. Zhang, L., et al., *Deep Potential Molecular Dynamics: A Scalable Model with the Accuracy of Quantum Mechanics.* Physical Review Letters, 2018. **120**(14): p. 143001.
8. Kresse, G. and J. Furthmüller, *Efficient iterative schemes for ab initio total-energy calculations using a plane-wave basis set.* Physical Review B, 1996. **54**(16): p. 11169-11186.
9. Kresse, G. and J. Hafner, *Ab initio molecular-dynamics simulation of the liquid-metal--amorphous-semiconductor transition in germanium.* Physical Review B, 1994. **49**(20): p. 14251-14269.
10. Blöchl, P.E., *Projector augmented-wave method.* Physical Review B, 1994. **50**(24): p. 17953-17979.
11. Zhang, L., et al., *End-to-end Symmetry Preserving Inter-atomic Potential Energy Model for Finite and Extended Systems*. 2018.
12. Wang, H., et al., *DeePMD-kit: A deep learning package for many-body potential energy representation and molecular dynamics.* Computer Physics Communications, 2018. **228**: p. 178-184.
13. Liang, W., G. Lu, and J. Yu, *Molecular dynamics simulations of molten magnesium chloride using machine learning-based deep potential(Advanced theory and simulations).* 2020. **3**.
14. Bu, M., et al., *Local structure elucidation and properties prediction on KCl–CaCl2 molten salt: A deep potential molecular dynamics study.* Solar Energy Materials and Solar Cells, 2021. **232**: p. 111346.
15. Adhikari, P., et al., *Electronic structure and mechanical properties of crystalline precipitate phases M23C6 (M = Cr, W, Mo, Fe) in Ni-based superalloys.* Materials Research Express, 2019. **6**.
16. Liu, Y., et al., *Mechanical properties and electronic structures of M23C6 (M = Fe, Cr, Mn)-type multicomponent carbides.* Journal of Alloys and Compounds, 2015. **648**: p. 874-880.
17. Jong, M., et al., *Charting the complete elastic properties of inorganic crystalline compounds.* Scientific Data, 2015. **2**.
18. Birch, F., *Finite Elastic Strain of Cubic Crystals.* Physical Review, 1947. **71**(11): p. 809-824.
19. Murnaghan, F.D., *The Compressibility of Media under Extreme Pressures.* Proceedings of the National Academy of Sciences, 1944. **30**(9): p. 244.
20. Hirel, P., *Atomsk: A tool for manipulating and converting atomic data files.* Computer Physics Communications, 2015. **197**: p. 212-219.

Graphical Abstract